

Quark deconfinement transition in hyperonic matter

Toshiki Maruyama,¹ Satoshi Chiba,¹ Hans-Josef Schulze,²
and Toshitaka Tatsumi³

¹ *Advanced Science Research Center, Japan Atomic Energy Agency, Tokai, Ibaraki 319-1195, Japan*

² *INFN Sezione di Catania, Via Santa Sofia 64, I-95123 Catania, Italy*

³ *Department of Physics, Kyoto University, Kyoto 606-8502, Japan*

Abstract

We discuss the properties of the hadron-quark mixed phase in compact stars using a realistic equation of state of hyperonic matter and the MIT bag model. We find that the equation of state of the mixed phase is similar to that given by the Maxwell construction, but that the mixed phase becomes mechanically unstable if the surface tension of the interface between the two pure phases is strong enough. The composition of the mixed phase is very different from that of the Maxwell construction; in particular, hyperons are completely suppressed.

It is commonly believed that hyperons appear in dense nuclear matter at baryon densities above 2–3 times normal density, in spite of some uncertainties about the nucleon-hyperon (NY) and hyperon-hyperon (YY) interactions. Many theoretical studies have shown that the hadronic equation of state (EOS) becomes very soft once hyperons become components of the matter [1, 2]. As a major consequence, the maximum mass of neutron stars (NS) predicted using the hyperonic EOS may remain below the current observational values of about 1.5 solar masses [3].

Some authors have suggested that this situation might be remedied by considering the yet unknown three-body forces (TBF) among hyperons and nucleons [4], while other studies have shown that a quark deconfinement

phase transition in hyperonic matter renders the EOS sufficiently stiff again to allow NS masses consistent with current data [5].

However, the appearance of quark matter (QM) poses the problem of an accurate theoretical description of the quark phase, which is so far an open question, and furthermore of the details of the phase transition between hadronic and quark matter. The purpose of this letter is the study of the latter problem, combining a Brueckner-Hartree-Fock (BHF) EOS of hyperonic hadronic matter with the standard phenomenological MIT model for the quark phase. In the simplest scenario, the Maxwell construction (MC), a sharp transition takes place between the two charge-neutral hadron and quark phases, whereas the more general Gibbs (Glendenning) construction (GC) [6] allows a mixed phase (MP) containing individually charged hadron and quark fractions with various geometrical structures. However, in the latter case, electromagnetic and surface contributions to the energy of the MP are usually neglected, but could have important effects [7, 8, 9]. The quantitative analysis of these corrections is the purpose of this letter.

Our theoretical framework for the hadronic matter is the nonrelativistic BHF approach [2, 10] based on microscopic NN, NY, and YY potentials that are fitted to scattering phase shifts, where possible. Nucleonic three-body forces (TBF) are included in order to (slightly) shift the saturation point of purely nucleonic matter to the empirical value. It has been demonstrated that the theoretical basis of the BHF method, the hole-line expansion, is well founded: the nuclear EOS can be calculated with good accuracy in the BHF two hole-line approximation with the continuous choice for the single-particle potential, since the results in this scheme are quite close to the full convergent calculations which include also the three hole-line contributions [10, 11]. Due to these facts, combined with the absence of adjustable parameters, the BHF model is a reliable and well-controlled theoretical approach for the study of dense baryonic matter.

The basic input quantities in the Bethe-Goldstone equation are the NN, NY, and YY potentials. In this work we use the Argonne V_{18} NN potential [12] supplemented by the Urbana UIX nucleonic TBF of Refs. [13] and the Nijmegen soft-core NSC89 NY potentials [14] that are well adapted to the existing experimental NY scattering data and also compatible with Λ hypernuclear levels [15, 16]. With these potentials, the various G -matrices are evaluated by solving numerically the Bethe-Goldstone equation. Then the

total nonrelativistic hadronic energy density, ϵ_H , can be evaluated:

$$\epsilon_H = \sum_{i=n,p,\Lambda,\Sigma^-} \sum_{k < k_F^{(i)}} \left[T_i(k) + \frac{1}{2} U_i(k) \right], \quad (1)$$

with $T_i(k) = m_i + k^2/2m_i$, where the various single-particle potentials are given by

$$U_i(k) = \sum_{i'=n,p,\Lambda,\Sigma^-} U_i^{(i')}(k) \quad (2)$$

and are determined self-consistently from the G -matrices.

For the quark EOS, we use the MIT bag model with massless u and d quarks and massive s quark with $m_s = 150$ MeV. The quark matter energy density can be expressed as a sum of the kinetic term and the leading-order one-gluon-exchange term [17, 18] for the interaction energy proportional to the QCD fine structure constant α_s ,

$$\epsilon_Q = B + \sum_f \epsilon_f, \quad (3)$$

$$\begin{aligned} \epsilon_f(\rho_f) = & \frac{3m_f^4}{8\pi^2} \left[(2x_f^3 + x_f) \sqrt{1 + x_f^2} - \operatorname{arsinh} x_f \right] \\ & - \alpha_s \frac{m_f^4}{\pi^3} \left[x_f^4 - \frac{3}{2} (x_f \sqrt{1 + x_f^2} - \operatorname{arsinh} x_f)^2 \right], \end{aligned} \quad (4)$$

where m_f is the $f = u, d, s$ current quark mass, $x_f = k_F^{(f)}/m_f$, the baryon density of f quarks is $\rho_f = k_F^{(f)3}/3\pi^2$, and the bag constant B is the energy density difference between the perturbative vacuum and the true vacuum.

This is clearly an oversimplified model of QM, which will be used in this letter to study the generic qualitative features of the hadron-quark phase transition in NS matter. In future work we will compare in more detail the quantitative results obtained using different, more sophisticated, QM models.

Figure 1 compares the hadronic BHF EOS and the quark matter EOS with different values of the parameters B and α_s for beta-stable and charge-neutral matter. One can see that the quark EOS approaches that of a relativistic free gas ($E/A \sim \rho_B^{1/3}$) with increasing density, while the hyperonic EOS is always soft. Consequently the quark deconfinement transition cannot occur at too high densities. If we demand the quark and the hyperonic EOS to cross, α_s should be small and B slightly large, which gives a relatively low critical density. Thus the appearance of hyperons is effectively suppressed

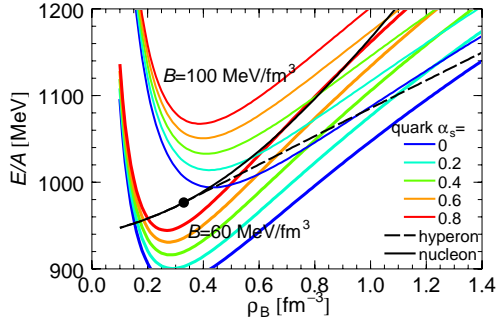


Figure 1: EOS of hadronic matter (black curves) and of quark matter (colored curves) with $B = 60 \text{ MeV/fm}^3$ (lower curves) and $B = 100 \text{ MeV/fm}^3$ (upper curves) for several values of α_s . Hyperons appear at the dotted point in hadronic matter.

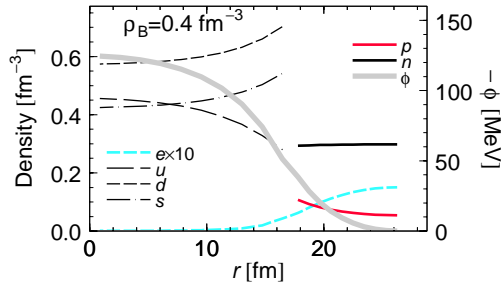


Figure 2: Density profiles and Coulomb potential ϕ within a 3D (quark droplet) Wigner-Seitz cell of the MP at $\rho_B = 0.4 \text{ fm}^{-3}$. The cell radius and the droplet radius are $R_W = 26.7 \text{ fm}$ and $R = 17.3 \text{ fm}$, respectively.

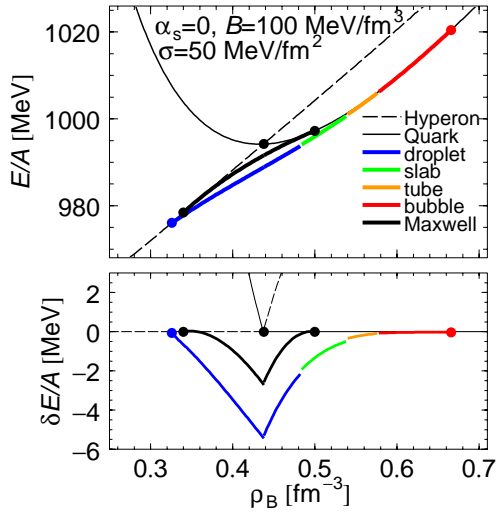


Figure 3: EOS of the MP (thick curves) in comparison with pure hadron and quark phases (thin curves). The upper panel shows the energy per baryon E/A and the lower panel the energy difference between mixed and hadron ($\rho_B < 0.44 \text{ fm}^{-3}$) or quark ($\rho_B > 0.44 \text{ fm}^{-3}$) phases. Different segments of the MP are chosen by minimizing the energy.

due to a quark deconfinement transition. In this letter we choose $\alpha_s = 0$ and $B = 100 \text{ MeV/fm}^3$.

The numerical procedure to determine the EOS and the geometrical structure of the MP is similar to that explained in detail in Refs. [9]. We employ a Wigner-Seitz approximation in which the whole space is divided into equivalent Wigner-Seitz cells with a given geometrical symmetry, sphere for three dimension (3D), cylinder for 2D, and slab for 1D. A lump portion made of one phase is embedded in the other phase and thus the quark and hadron phases are separated in each cell. A sharp boundary is assumed between the two phases and the surface energy is taken into account in terms of a surface-tension parameter σ . We use the Thomas-Fermi approximation for the density profiles of hadrons and quarks, while the Poisson equation for the Coulomb potential ϕ is explicitly solved. The energy density of the mixed phase is thus written as

$$\epsilon_M = \frac{1}{V_W} \left[\int_{V_H} d^3r \epsilon_H(\mathbf{r}) + \int_{V_Q} d^3r \epsilon_Q(\mathbf{r}) + \int_{V_W} d^3r \left(\epsilon_L(\mathbf{r}) + \frac{(\nabla\phi(\mathbf{r}))^2}{8\pi e^2} \right) + \sigma S \right], \quad (5)$$

where the volume of the Wigner-Seitz cell V_W is the sum of those of hadron and quark phases V_H and V_Q , and S the quark-hadron interface area. ϵ_L indicates the kinetic energy density of lepton (only the electron in this work). The energy densities ϵ_H , ϵ_Q and ϵ_L are \mathbf{r} -dependent since they are functions of local densities $\rho_a(\mathbf{r})$ ($a = n, p, \Lambda, \Sigma^-, u, d, s, e$). For a given density ρ_B , the optimum dimensionality of the cell, the cell size R_W , the lump size R , and the density profile of each component are searched for to give the minimum energy density. The structure of the MP changes from quark droplet to quark slab to hadron tube to hadron bubble with increasing baryon density.

The surface tension of the hadron-quark interface is poorly known, but some theoretical estimates based on the MIT bag model for strangelets [17] and lattice gauge simulations at finite temperature [19] suggest a range of $\sigma \approx 10\text{--}100 \text{ MeV/fm}^2$. We show results using $\sigma = 50 \text{ MeV/fm}^2$ in the present letter, and discuss the effects of its variation.

Figure 2 illustrates the outcome of this procedure, showing the density profile in a 3D cell for $\rho_B = 0.4 \text{ fm}^{-3}$. One can see the non-uniform density distribution of each particle species together with the finite Coulomb potential. The quark phase is negatively charged, so that d and s quarks are repelled to the phase boundary, while u quarks gather at the center. The protons in the hadron phase are attracted by the negatively charged quark

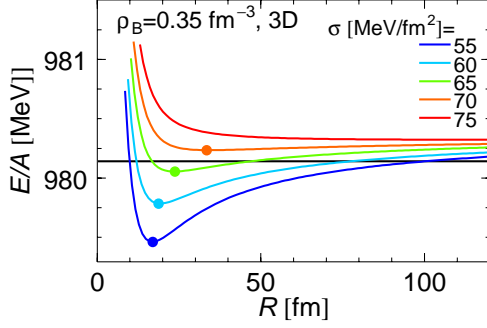


Figure 4: Droplet radius (R) dependence of the energy per baryon for fixed baryon density $\rho_B = 0.35 \text{ fm}^{-3}$ and different surface tensions. The quark volume fraction $(R/R_W)^3$ is fixed for each curve. Dots on the curves show the local energy minima. The black line shows the energy of the MC case.

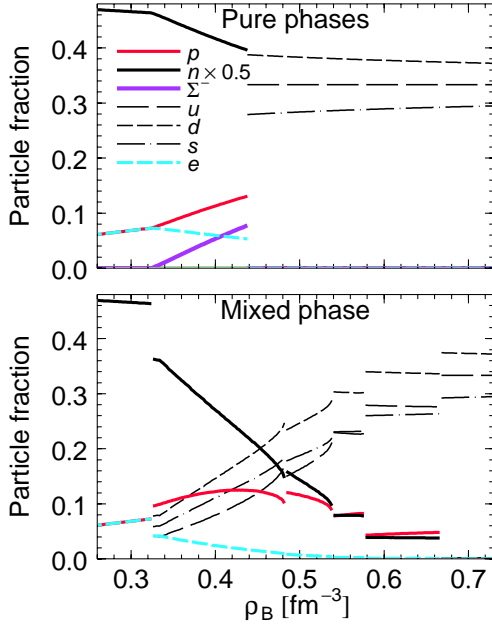


Figure 5: Particle fractions of quark and hadron species in the pure hadron and quark phases (upper panel) and in the MP (lower panel). In the MC the phase transition occurs between the pure phases with $\rho_B = 0.34 \text{ fm}^{-3}$ (hadrons) and 0.50 fm^{-3} (quarks).

phase, while the electrons are repelled.

Figure 3 (upper panel) compares the resulting energy per baryon of the hadron-quark MP with that of the pure hadron and quark phases over the relevant range of baryon density. The thick black curve indicates the case of the Maxwell construction, while the colored line indicates the MP in its various geometric realizations, starting at $\rho_B = 0.326 \text{ fm}^{-3}$ with a quark droplet structure and ending at $\rho_B = 0.666 \text{ fm}^{-3}$ with a hadron bubble structure. The energy of the MP is only slightly lower than that of the MC, and the resultant EOS is similar to the MC one. However, the structure and the composition of the MP are very different from those of the MC case, as discussed later.

If one uses a smaller surface tension parameter σ , the energy gets lower and the density range of the MP gets wider. The limit of $\sigma = 0$ leads to a bulk application of the Gibbs conditions without the Coulomb and surface effects, i.e., the so-called Glendenning construction [6]. On the other hand, using a larger value of σ , the geometrical structures increase in size and the EOS gets closer to that of the MC case. Above a limiting value of $\sigma \approx 65 \text{ MeV}/\text{fm}^2$ the structure of the MP becomes mechanically unstable [8]: for a fixed volume fraction $(R/R_W)^3$ the optimal values of R and R_W go to infinity and local charge neutrality is recovered in the MP, where the energy density equals that of the MC (see Fig. 4).

This mechanical instability is due to the charge screening effect: The optimal values of R and R_W are basically determined by the balance between the Coulomb energy ($\sim R^2$ in the 3D case) and the surface energy ($\sim R^{-1}$). However, if the charge screening is taken into account, the contribution of the screened Coulomb potential ϕ is strongly reduced when $R, R_W \rightarrow \infty$. A careful analysis by Voskresensky et al. showed that the Coulomb energy changes its sign and behaves like R^{-1} as $R \rightarrow \infty$ due to the charge screening effect [8]. Thus the surface and the Coulomb energy give a local minimum below $\sigma \approx 65 \text{ MeV}/\text{fm}^2$, which disappears when the surface energy becomes greater than the Coulomb energy above $\sigma \approx 65 \text{ MeV}/\text{fm}^2$. This is in contrast to the work of Heiselberg et al. [7], neglecting the charge screening effect, where there is always a local energy minimum at finite R . The importance of the charge screening effect has been also shown in the stability of strangelets [20].

One notes in Fig. 2 that no hyperons appear in the MP although the mean baryon density $\rho_B = 0.4 \text{ fm}^{-3}$ is higher than the threshold density for hyperons in pure nucleon matter $\rho_B = 0.34 \text{ fm}^{-3}$ (see the black dot in Fig. 1).

In the upper panel, the case of the pure hadron and quark phases is shown for comparison. One can see that the particle fractions are very different in both cases, in particular a relevant hyperon fraction is only present in the hadronic part of the MC.

Thus we conclude that due to the relatively small magnitudes of the surface and Coulomb energies, the EOS of the MP is similar to the MC one, but the internal structure of the MP is very different. In particular the role of hyperons is strongly reduced when we consider the deconfinement transition in hyperonic matter. Above a maximum value of the surface tension parameter, the MC is recovered as the physical one, however. These results should be important for physical processes like neutrino propagation and baryonic superfluidity, besides the maximum mass problem, which will be studied in an extended article.

This work is partially supported by the Grant-in-Aid for the 21st Century COE “Center for the Diversity and Universality in Physics” and the Grant-in-Aid for Scientific Research Fund of the Ministry of Education, Culture, Sports, Science and Technology of Japan (13640282, 16540246).

References

- [1] N. K. Glendenning, *Compact Stars: Nuclear Physics, Particle Physics and General Relativity*, 2nd ed. (Springer, Berlin, 2000); F. Weber, *Pulsars as Astrophysical Laboratories for Nuclear and Particle Physics* (IOP Publishing, Bristol, 1999).
- [2] M. Baldo, G. F. Burgio, and H.-J. Schulze, *Phys. Rev.* **58**, 3688 (1998); *Phys. Rev.* **61**, 055801 (2000); H.-J. Schulze, A. Polls, A. Ramos, and I. Vidaña, *Phys. Rev.* **C73**, 058801 (2006).
- [3] For a recent review, see D. Page and S. Reddy, *Annu. Rev. Nucl. Part. Sci.* **56**, 327 (2006).
- [4] S. Nishizaki, Y. Yamamoto, and T. Takatsuka, *Prog. Theor. Phys.* **105**, 607 (2001); **108**, 703 (2002).
- [5] G. F. Burgio, M. Baldo, P. K. Sahu, and H.-J. Schulze, *Phys. Rev.* **C66**, 025802 (2002); M. Baldo, M. Buballa, G. F. Burgio, F. Neumann, M. Oertel, and H.-J. Schulze, *Phys. Lett.* **B562**, 153 (2003); C. Maieron,

- M. Baldo, G. F. Burgio, and H.-J. Schulze, Phys. Rev. **D70**, 043010 (2004).
- [6] N. K. Glendenning, Phys. Rev. **D46**, 1274 (1992); Phys. Rep. **342**, 393 (2001).
- [7] H. Heiselberg, C. J. Pethick, and E. F. Staubo, Phys. Rev. Lett. **70**, 1355 (1993); N. K. Glendenning and S. Pei, Phys. Rev. **C52**, 2250 (1995); M. B. Christiansen and N. K. Glendenning, Phys. Rev. **C56**, 2858 (1997); N. K. Glendenning, Phys. Rep. **342**, 393 (2001).
- [8] D. N. Voskresensky, M. Yasuhira, and T. Tatsumi, Phys. Lett. **B541**, 93 (2002); Nucl. Phys. **A723**, 291 (2003); T. Tatsumi, M. Yasuhira, and D. N. Voskresensky, Nucl. Phys. **A718**, 359 (2003).
- [9] T. Endo, T. Maruyama, S. Chiba, and T. Tatsumi, Nucl. Phys. **A749**, 333 (2005); T. Endo, T. Maruyama, S. Chiba, and T. Tatsumi, Prog. Theor. Phys. **115**, 337 (2006); T. Maruyama, T. Tatsumi, T. Endo, and S. Chiba, Recent Res. Devel. in Physics **7**, 1 (2006).
- [10] M. Baldo, *Nuclear Methods and the Nuclear Equation of State* (World Scientific, Singapore, 1999).
- [11] H. Q. Song, M. Baldo, G. Giansiracusa, and U. Lombardo, Phys. Rev. Lett. **81**, 1584 (1998); M. Baldo, G. Giansiracusa, U. Lombardo, and H. Q. Song, Phys. Lett. **B473**, 1 (2000); M. Baldo, A. Fiasconaro, H. Q. Song, G. Giansiracusa, and U. Lombardo, Phys. Rev. **C65**, 017303 (2002); R. Sartor, Phys. Rev. **C73**, 034307 (2006).
- [12] R. B. Wiringa, V. G. J. Stoks, and R. Schiavilla, Phys. Rev. **C51**, 38 (1995).
- [13] B. S. Pudliner, V. R. Pandharipande, J. Carlson, S. C. Pieper, and R. B. Wiringa, Phys. Rev. **C56**, 1720 (1997); M. Baldo, I. Bombaci, and G. F. Burgio, Astron. Astroph. **328**, 274 (1997); M. Baldo and L. S. Ferreira, Phys. Rev. **C59**, 682 (1999); X. R. Zhou, G. F. Burgio, U. Lombardo, H.-J. Schulze, and W. Zuo, Phys. Rev. **C69**, 018801 (2004).
- [14] P. M. M. Maessen, Th. A. Rijken, and J. J. de Swart, Phys. Rev. **C40**, 2226 (1989).

- [15] Th. A. Rijken, V. G. J. Stoks, and Y. Yamamoto, Phys. Rev. **C59**, 21 (1999).
- [16] J. Cugnon, A. Lejeune, and H.-J. Schulze, Phys. Rev. **C62**, 064308 (2000); I. Vidaña, A. Polls, A. Ramos, and H.-J. Schulze, Phys. Rev. **64**, 044301 (2001).
- [17] E. Farhi and R. L. Jaffe, Phys. Rev. **D30**, 2379 (1984); M. S. Berger and R. L. Jaffe, Phys. Rev. **C35**, 213 (1987).
- [18] R. Tamagaki and T. Tatsumi, Prog. Theor. Phys. Suppl. **112**, 277 (1993).
- [19] K. Kajantie, L. Kärkäinen, and K. Rummukainen, Nucl. Phys. **B357**, 693 (1991); S. Huang, J. Potvion, C. Rebbi, and S. Sanielevici, Phys. Rev. **D42**, 2864 (1990); **D43**, 2056 (1991).
- [20] H. Heiselberg, Phys. Rev. **D48**, 1418 (1993).
P. Jaikumar, S. Reddy and A. W. Steiner, Phys. Rev. Lett. **96**, 040011 (2006); M. G. Alford, K. Rajagopal, S. Reddy and A. W. Steiner, Phys. Rev. **D73**, 114016 (2006).